STRUCTURE OF GALAXIES

5. Kinematics of galaxies

Piet van der Kruit
Kapteyn Astronomical Institute
University of Groningen
the Netherlands

February 2010

HI in spiral galaxies

HI observations

As an example I take the observations of NGC 3198 with the Westerbork Synthesis Radio Telescope.

These observations are part of the Palomar-Westerbork Survey of northern spiral galaxies[1].

This survey combined 21-cm observations of the neutral hydrogen with three-color optical surface photometry from photographic plates with the Palomar 48-inch Schmidt-telescope.

[1]B.M.H.R. Wevers, Ph.D. Thesis, 1984, B.M.H.R. Wevers, P.C. van der Kruit & R.J Allen, A.&A.Suppl. 66, 505 (1986)

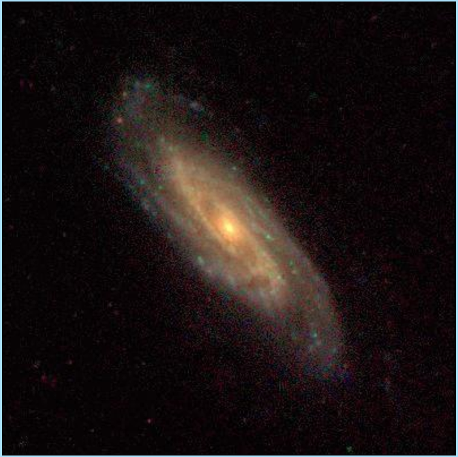

HI observations are done in narrow frequency channels with widths of order ten or a few tens of km/s.

The first thing to do is add up the channels at which no HI is present to find the continuum map.

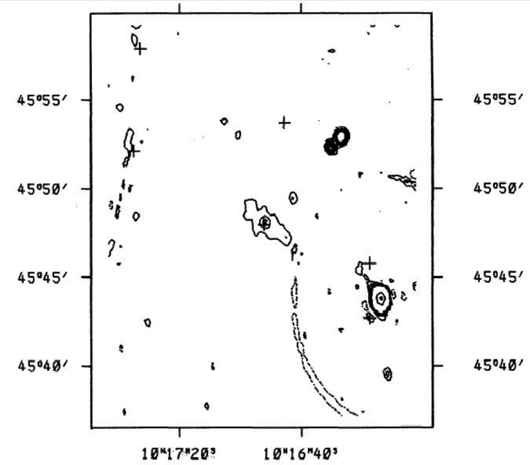

The continuum radiation is mostly non-thermal synchrotron emission from relativistic electrons moving in the galactic magnetic field.

At the position of the HII-regions there also is thermal free-free emission from interaction between free electrons and ionized hydrogen (protons).

This particular galaxy has radio emission from the center and some extended faint emission from the disk.

This continuum map is then subtracted from all channel maps to reveal the distribution of HI at various velocities.

The continuum map should be produced from as many channel maps as possible, so that the noise in it is low compared to that in the channel maps themselves.

Here are the channel maps of NGC 3198 as far as they contain neutral hydrogen emission.

The radial velocity increases from left-top (468 km sec^{-1}) to right-bottom (832 km sec^{-1}) in steps of 33 km sec^{-1}.

Obviously the northern (top) part is approaching us with respect to the systemic velocity and the southern part is receeding.

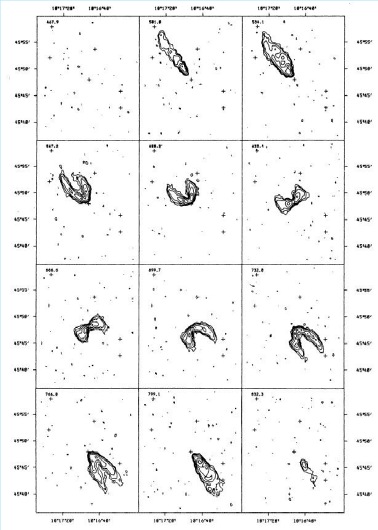

These channel maps can be added to produce the map with the distribution of neutral hydrogen, the total HI-map.

To suppress noise usually this is preceded by blocking out the areas in each of the channel maps that appear to have no HI-signal and thus contain only noise.

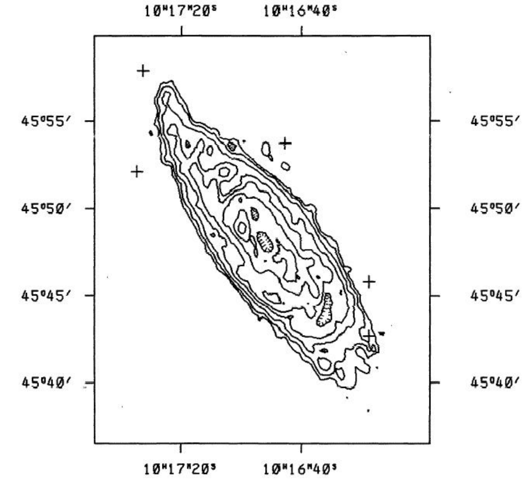

Analysis of HI observations

From this map the radial HI profile can be produced by averaging in azimuthal annuli.

In practice this is done after analysis of the velocity field in order to find the position of the center and the orientation parameters (direction of major axis and inclination).

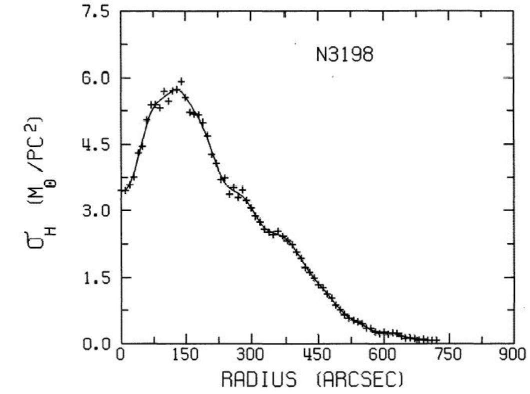

One can then take the optical map(s) and derive the radial luminosity profiles.

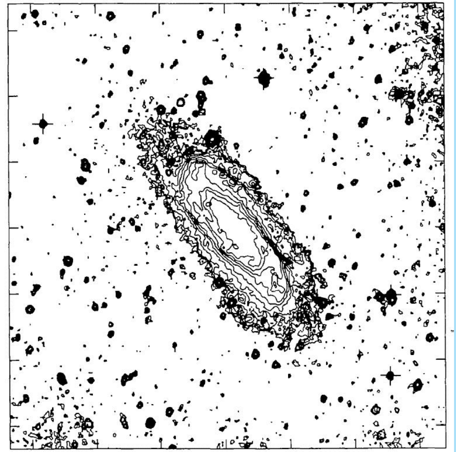

These can be further extended with radial color profiles and radial profile of the HI-surface density versus optical surface luminosity.

Here we have on the left from top to bottom the surface brightness profiles in three color bands, the radial profiles of three color indices and ratio of the (face-on) surface density if HI over the surface brightnes.

On the right are azimuthal color profiles and at the bottom differences of surface brightnesses from independent meassurements (not applicable here).

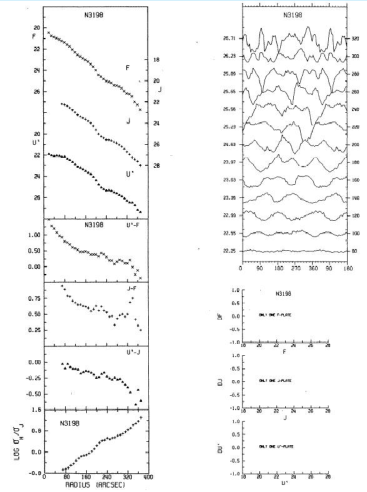

The profiles are tabulated here.

The units are magnitudes per arcsec^2 for surface brightness (or equivalently in solar luminosities per pc^2), magnitudes for color, solar masses per pc^2 for HI-surface densities and solar masses over solar luminosities for the density–brightness ratio.

NGC 3198 surface brightness

radius arcsec	U'	J	F	U'-J	J-F	U'-F
0.	-	-	-	-	-	-
10.	-	-	-	-	-	-
20.	21.91	-	20.43	-	-	1.48
30.	22.03	-	20.75	-	-	1.28
40.	22.08	-	20.88	-	-	1.20
50.	22.04	-	20.97	-	-	1.07
60.	22.07	-	21.10	-	-	0.97
70.	22.16	22.19	21.24	-0.03	0.95	0.92
80.	22.15	22.25	21.36	-0.10	0.89	0.79
90.	22.35	22.38	21.59	-0.03	0.79	0.76
100.	22.46	22.54	21.76	-0.08	0.78	0.70
110.	22.65	22.76	22.05	-0.11	0.71	0.60
120.	22.88	22.99	22.31	-0.11	0.68	0.57
130.	23.08	23.20	22.55	-0.12	0.65	0.53
140.	23.18	23.36	22.71	-0.18	0.65	0.47
150.	23.33	23.49	22.86	-0.16	0.63	0.47
160.	23.49	23.63	23.01	-0.14	0.62	0.48
170.	23.64	23.79	23.19	-0.15	0.60	0.45
180.	23.80	23.97	23.42	-0.17	0.55	0.38
190.	24.05	24.25	23.67	-0.20	0.58	0.38
200.	24.39	24.64	24.01	-0.25	0.63	0.38
210.	24.76	25.00	24.44	-0.24	0.56	0.32
220.	25.05	25.24	24.62	-0.19	0.62	0.43
230.	25.22	25.39	24.83	-0.17	0.56	0.39
240.	25.33	25.56	25.03	-0.23	0.53	0.30
250.	25.31	25.57	25.11	-0.26	0.46	0.20
260.	25.37	25.65	25.18	-0.28	0.47	0.19
270.	25.51	25.76	25.43	-0.25	0.33	0.08
280.	25.60	25.88	25.45	-0.28	0.43	0.15
290.	25.77	26.04	25.56	-0.27	0.48	0.21
300.	25.89	26.21	25.71	-0.32	0.50	0.18
310.	26.08	26.44	25.98	-0.36	0.46	0.10
320.	26.30	26.70	26.20	-0.40	0.50	0.10
330.	26.46	26.94	26.25	-0.48	0.69	0.21
340.	26.47	27.24	26.49	-0.77	0.75	-0.02
350.	26.74	27.41	26.99	-0.67	0.42	-0.25
360.	27.15	27.59	27.27	-0.44	0.32	-0.12
370.	27.37	27.98	27.73	-0.61	0.25	-0.36

NGC 3198 HI surface density

radius arcsec	σ(HI) $M_\odot/pc^2$	σ(J) $L_\odot/pc^2$	LOG(σ(HI)/σ(J)) $M_\odot/L_\odot$
0.	3.453	-	-
30.	3.758	-	-
60.	5.039	-	-
90.	5.312	20.800	-.593
120.	5.706	11.859	-.318
150.	5.553	7.483	-.129
180.	5.154	4.809	.030
210.	4.262	5.862	.360
240.	3.741	1.112	.527
270.	3.299	.925	.552
300.	3.057	.611	.699
330.	2.586	.312	.919
360.	2.546	.171	1.172
390.	2.238	-	-
420.	1.723	-	-
450.	1.331	-	-
480.	1.024	-	-
510.	.656	-	-
540.	.499	-	-
570.	.355	-	-
600.	.271	-	-
630.	.236	-	-
660.	.132	-	-
690.	.105	-	-
720.	.081	-	-

The velocity field follows from deriving at each position the radial velocity.

This can be done either by moment analysis of the HI-profile or a fit with a Gaussian.

This is called a spider diagram.

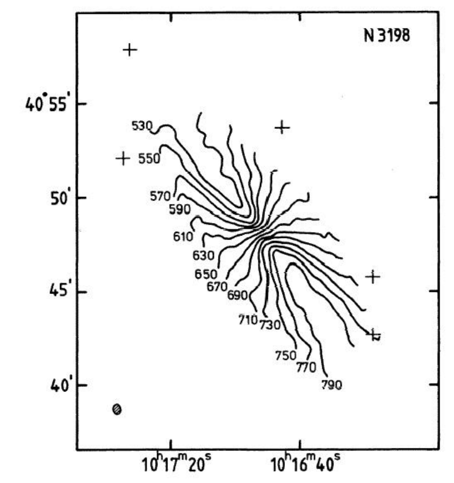

Helpful for further analysis are also position-velocity diagrams (or x,V-diagrams), which have position along a line (or curve) on one axis and radial velocity on the other.

The figure shows the x,V-diagrams along the major and minor axis.

Also useful is the integrated profile.

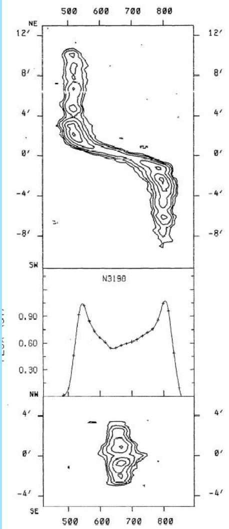

The next step is to analyse the velocity field in terms of the orientation of the plane of the disk and the rotation curve.

A first guess for the major axis direction and the inclination can be obtained from the distribution of HI and/or the optical image.

Assume we have a disk galaxy with a rotation curve $V_{\rm rot}(R)$.
The position angle of the major axis is $\Phi_\circ$ and the inclination is i (defined as zero for face-on).
Take the coordinates on the sky as (r, Φ) and in the plane of the galaxy (R, θ). Then

$$R = r\frac{\cos(\Phi - \Phi_\circ)}{\cos\theta} \qquad \tan\theta = \frac{\tan(\Phi - \Phi_\circ)}{\cos i}$$

$$V_{\rm obs} = V_{\rm sys} + V_{\rm rot}(R)\sin i\cos\theta$$

We can calculate the pattern of the residual velocity field after subtraction of a model.

We then see that errors in each parameter produce different patterns and therefore in principle these parameters can be determined independently[a].

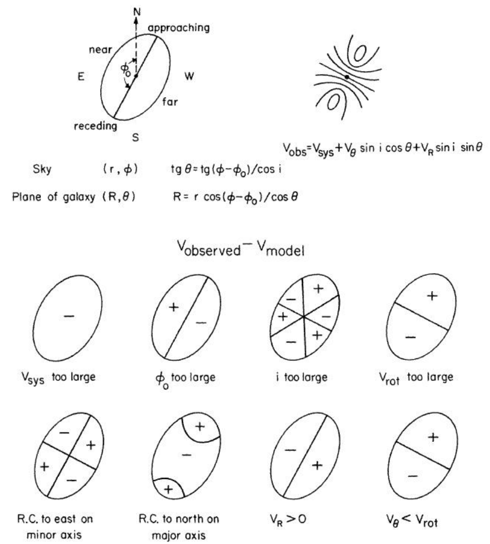

[a] see P.C. van der Kruit & R.J Allen, Ann.Rev.Astron.Astrophys. 16, 103 (1978)

The usual procedure to determine the velocity field is as follows.

From the optical maps the position of the center, the position angle of the major axis and the inclination are estimated.

Then in rings in the galaxy plane (which corresponds to ellipses on the sky) the observed velocities are converted into “rotation velocities” along the ring.

Then changes in the parameters are introduced; this changes the run of deduced rotation velocity along the ring.

The parameters are optimized until these variations along the ring are minimal.

In practice it turns out that in particular in the outer regions the planes of the rings change.

Example of an inclined galaxy: NGC 5055

This is illustrated with the observations of NGC 5055[2].

[2] A. Bosma, Ph.D. thesis, 1978; A.J. 86, 1791 (1981)

Here is the ditribution of HI.

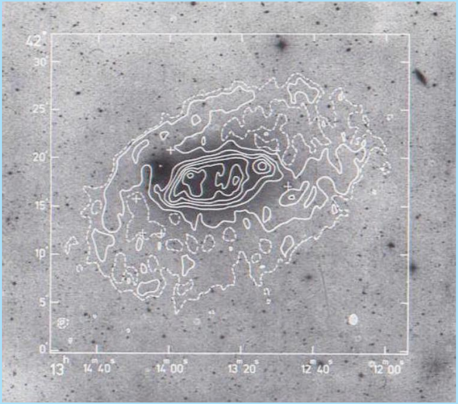

The distribution of the HI in the outer parts suggests that the plane of the disk changes. This is called a "warp".

We also see distortions in the velocity field.

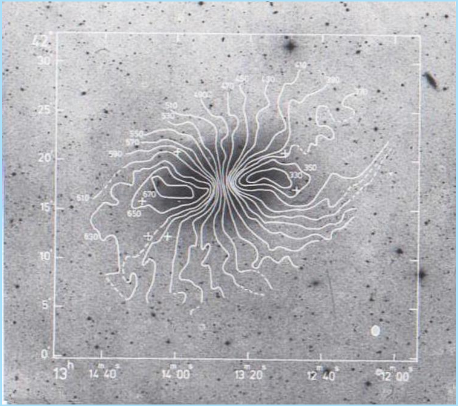

The velocity field is conveniently represented in color (from Albert Bosma's thesis):

The distribution and velocity field of the HI can be fitted with "inclined rings" with pure rotation in a changing plane.

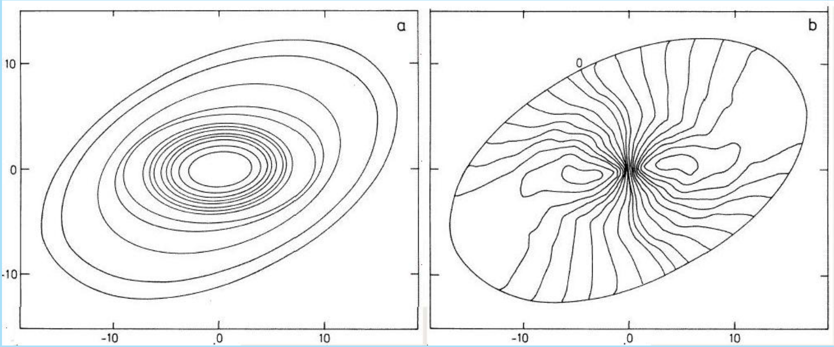

The figure shows from top to bottom:

Position angle of the major axis

Inclination

Rotation velocity

We return to the matter of warps later.

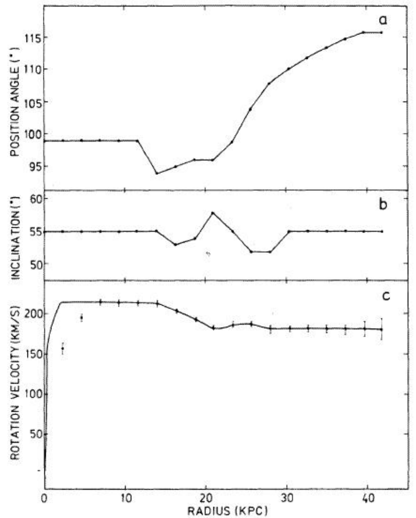

Example of an edge-on galaxy: NGC 891

The observations are from Sancisi & Allen[3].

[3] R. Sancisi & R.J. Allen, A.&A. 74, 73 (1979)

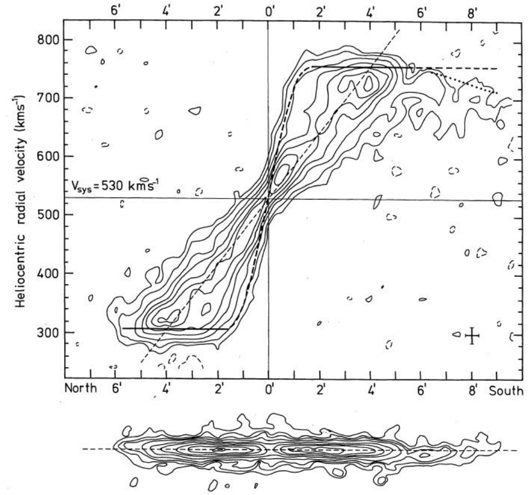
6'
4'
2'
0'
2'
4'
6'
8'
800
700
600
500
400
300
Heliocentric radial velocity (kms^{-1})
V_{sys} = 530 kms^{-1}
North
South

The position-velocity diagram (l, V-diagram) now is a projection of the plane of the galaxy with only a ambiguity around the "line of nodes".

This can be seen when we draw lines of equal line of sight velocity on the plane of the galaxy.

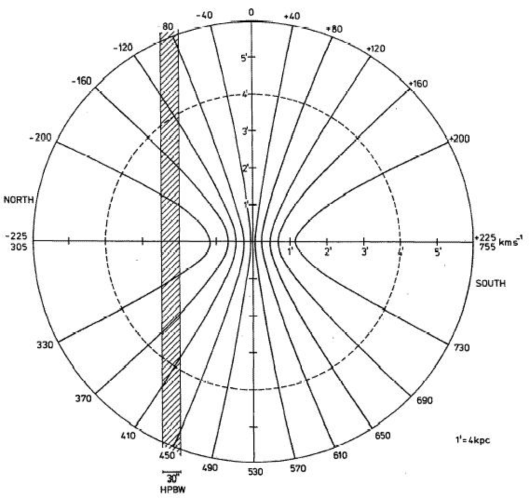

It is possible to model the I, V-diagram in terms of a distribution of the HI and a rotation curve.

The radial HI distribution can be estimated by “decomposing” the observed HI on the sky under the assumption of circular symmetry.

The “extreme” or “high” velocities give a first estimate of the rotation curve.

To properly model the I, V-diagram one needs to assume an HI velocity dispersion.

NGC 891 does not have an extended Hi disk beyond the stellar disk and the HI layer appears very flat.

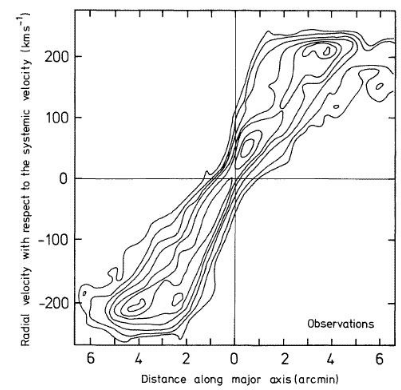
Radial velocity with respect to the systemic velocity (kms^{-1})
200
100
0
-100
-200
6
4
2
0
2
4
6
Distance along major axis (arcmin)
Observations

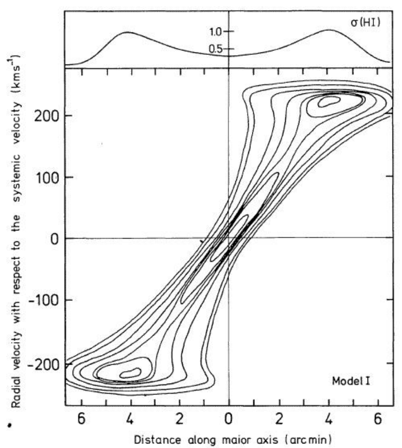
σ(HI)
1.0
0.5
Radial velocity with respect to the systemic velocity (kms^{-1})
200
100
0
-100
-200
6
4
2
0
2
4
6
Distance along major axis (arcmin)
Model I

The resulting rotation cuve is typical with a sharp rise and then remaining constant.

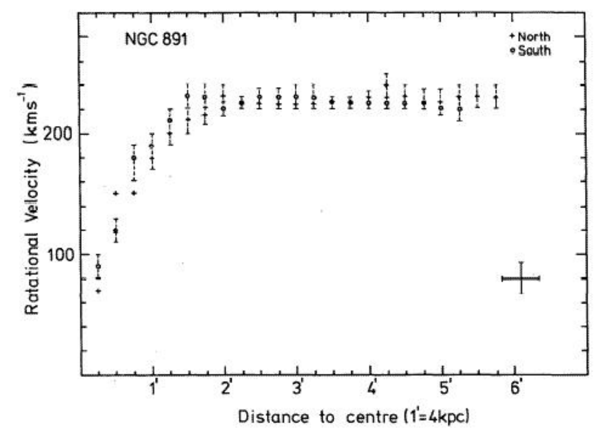

Warps

- Warps in the HI in external galaxies are most readily observed in edge-on systems as NGC 5907[4].

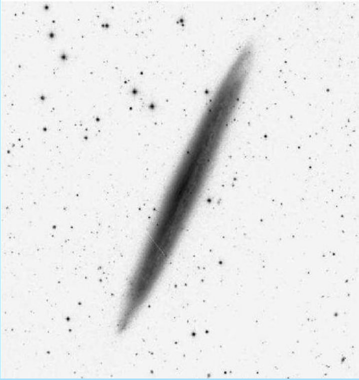

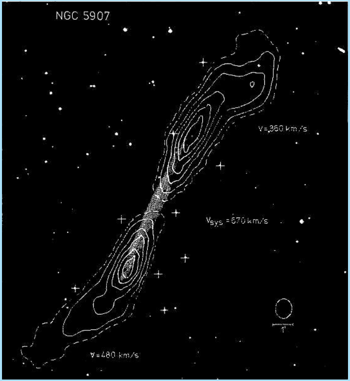

[4]R. Sancisi, A.&A. 74, 73 (1976)

- An extreme example is "prodigious warp" in NGC 4013[5].
- The warp is very symmetric and starts suddenly near the end of the optical disk (see the extreme channel maps on the left).

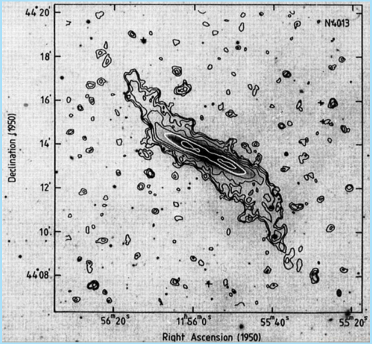

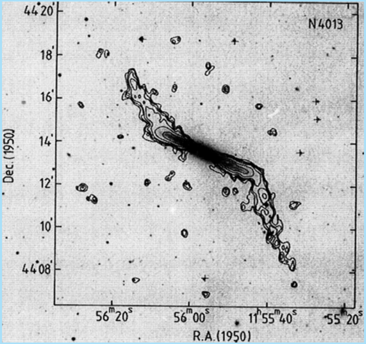

[5] R. Bottema, G.S.Shostak & P.C. van der Kruit, Nature 328, 401 (1987); R. Bottema, A.&A. 295, 605 (1995) and 306, 345 (1996)

- It is interesting to note that the NGC 5907 has a clear and sharp truncation[6] in its stellar disk, where also the warp starts.

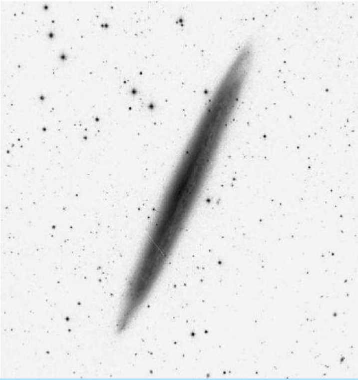

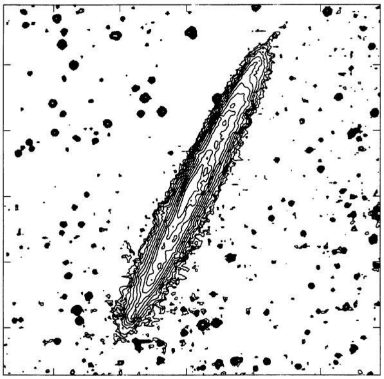

[6] P. C. van der Kruit & L. Searle, A.&A. 110, 61

- NGC 4013 also has a clear truncation[7] in its stellar disk. The three-dimensional analysis[8] does confirm that in deprojection the warp strats very close to the truncation radius.

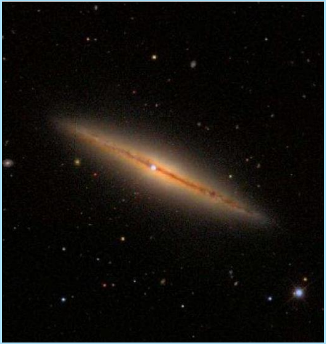

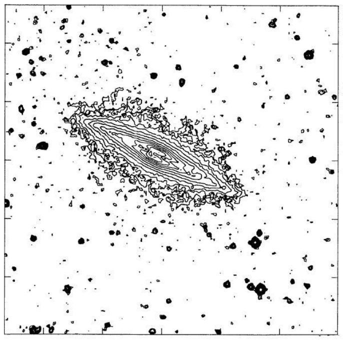

[7] P. C. van der Kruit & L. Searle, *op. cit.*

[8] R. Bottema, *op. cit.*

- Warps were already seen in less inclined systems, such as M83[9].
- These "kinematic warps" were fitted with so-called "tilted-ring models".

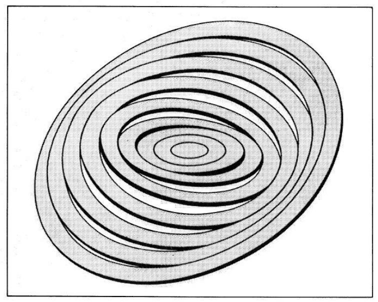

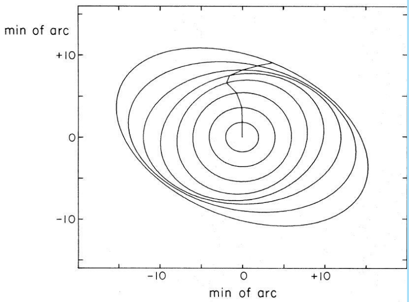

[9] D.H. Rogstad, I.A. Lockhart & M.C.H. Wright, Ap.J. 193, 309 (1974)

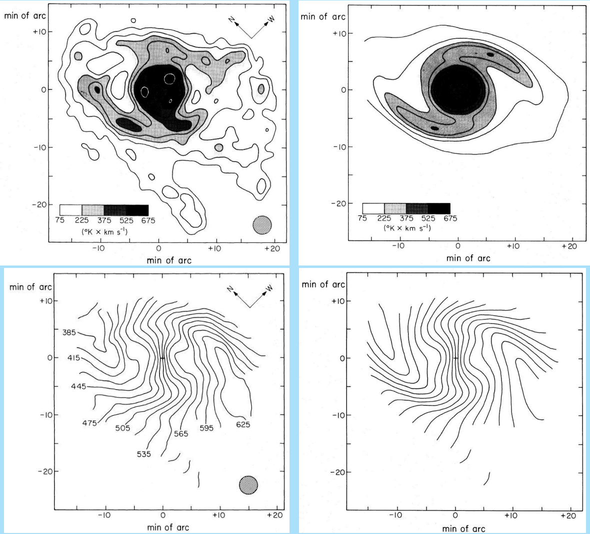
min of arc
+10
0
-10
-20
N
W
75 225 375 525 675
(°K × km s^{-1})
-10 0 +10 +20
min of arc
385
415
445
475
505
535
565
595
625

García Ruiz[10] has done a survey of edge-on galaxies.

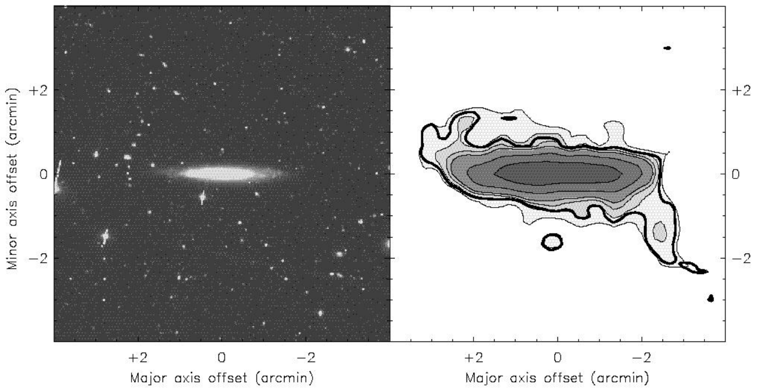

[10] I. García-Ruis, Ph.D. thesis (2001); I. García-Ruiz, R. Sancisi & K.H. Kuijken, A.&A. 394, 796 (2002)

His major findings are;

- All galaxies, in which the HI is more extended than the stellar disk have warps.
- The warp usually starts near the edge of the stellar disk.
- Galaxies in rich environments tend to have larger and more asymmetric warps.

- Briggs[11] formulated a set of rules of behaviour for HI- warps.

RULES OF BEHAVIOR FOR GALACTIC WARPS

F. H. BRIGGS
Kapetyn Astronomical Institute, University of Groningen, and Department of Physics and Astronomy, University of Pittsburgh
Received 1989 July 21; accepted 1989 September 19

ABSTRACT

A sample of galaxies is now available for which H I 21 cm line observations allow the development of detailed kinematic models based on concentric, circular rings with adjustable inclinations and orbital velocity. By examining these warped systems in a variety of reference frames, clear empirically determined "rules" for the behavior of galactic warps have emerged.

Analysis of 12 galaxies with extended, warped H I disks show the following:

1. The H I layer typically is planar within R_{25}, but warping becomes detectable within $R_{\rm Ho} = R_{26.5}$. Warping within $R_{\rm Ho}$ appears consistent with a common (i.e., straight) line of the nodes (LON) measured in the plane defined by the innermost regions of the galaxies.

2. Warps change character at a transition radius near $R_{\rm Ho}$.

3. For radii larger than $R_{\rm Ho}$, the LON measured in the plane of the inner galaxy advances in the direction of galaxy rotation for successively larger radii. Thus, the nodes lie along leading spirals in this frame of reference.

4. The galaxy kinematics uniquely specify a new reference frame in which there is a common LON for oribits within the transition radius and also a *differently oriented* straight LON for the gas outside the transition radius. This new reference frame is typically inclined by less than 10° to the plane of the inner galaxy.

The lack of a common LON throughout the entire warped disk argues against models that rely on normal bending modes to maintain warp coherence at all radii. Instead, the emerging picture may require galaxy models with two distinct regimes. Behavior in the outer regime is consistent with models that have the LON regressing most rapidly for oribits that are in closest proximity to the flat, stellar disk. In the inner regime, the disk may be settling into a warped mode.

---

[11] F.H. Briggs, Ap.J. 352, 15 (1990)

The most important aspects of Brigg's rules for the present discussion are:

- The HI layer typically is planar within R_{25}, but warping becomes detectable near $R_{Ho} = R_{26.5}$.
- Warps change character at a transition radius near R_{Ho}.
- The outer warp defines a reference frame.

A recent finding[a] indicates that warps start just beyond the truncation radius.

[a] P.C. van der Kruit, A.&A. 466, 883 (2007)

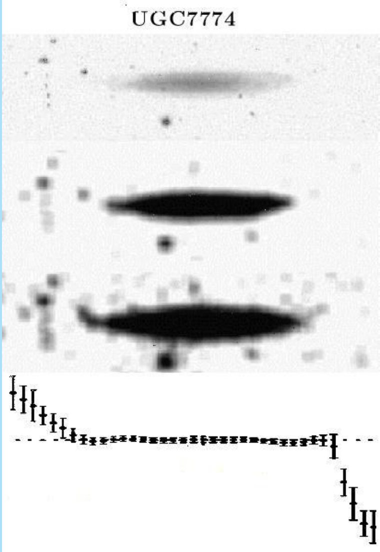

Properties of warps can be summarized as follows:

- All galaxies with extended HI disks have warps .
- Many galaxies have relatively sharp truncations.
- In edge-on galaxies the HI warps sets in just beyond the truncation radius, for less inclined systems it sets in near the Holmberg radius.
- In many cases the rotation curve shows a feature that indicates that there is at the truncation radius also a sharp drop in mass surface density.
- The onset of the warp is abrupt and discontinuous. and there is a steep slope in HI-surface density at this point.
- Inner disks are extremely flat and the warps define a single "new reference frame".

This may mean that the inner stellar disk formed first with a truncation and that the HI in the warp fell in later with another orientation of its angular momentum.

Often spiral galaxies are "lob-sided"[12] in their outer HI, such as NGC4395.

This has been explained as disks that are lying off-center in a dark halo[13].

[12] R.H.M. Schoenmakers, Ph.D. thesis (1999), R.S. Swaters, R.H.M. Schoenmakers, R. Sancisi & T.S. van Albada, Mon.Not.R.A.S. 304, 330 (1999)

[13] S.E. Levine & L.S. Sparke, Ap.J. 496, L13 (1998); E. Noordermeer, L.S. Sparke & S.E. Levine, Mon.Not.R.A.S. 328, 1064 (2001)

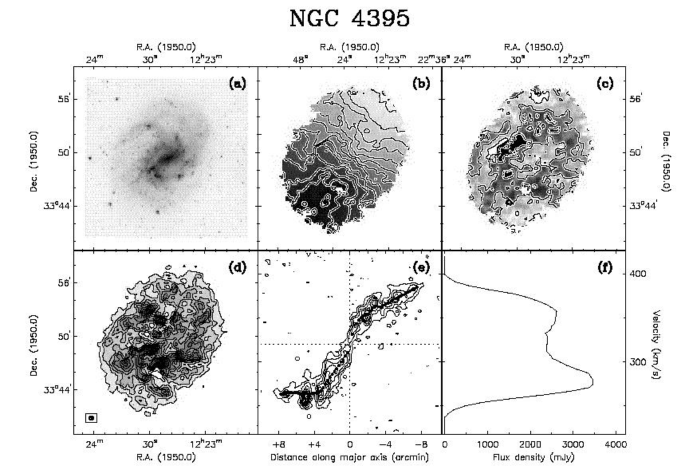

(panel c has residual velocities)

Velocity dispersions

NGC 628 is very close to face-on and can therefore be used to measure the velocity dispersion of the HI[14].

[14] G.S. Shostak & P.C. van der Kruit, A.&A. 132, 20 (1984)

The fact the NGC 628 is close to face-on is visible in the width of the integrated HI profile.

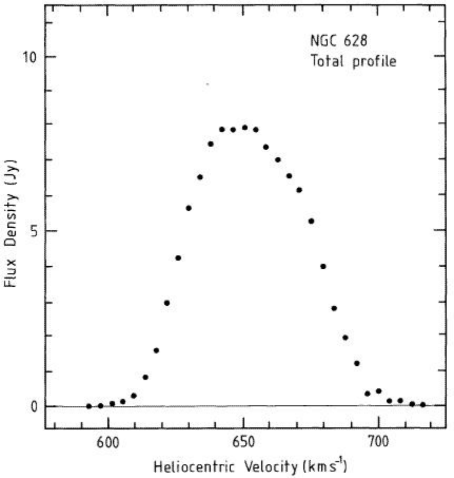

The HI is much more extended than the optical image.

Also the spiral strcuture continues in the HI beyond the stellar disk and the optical spiral arms.

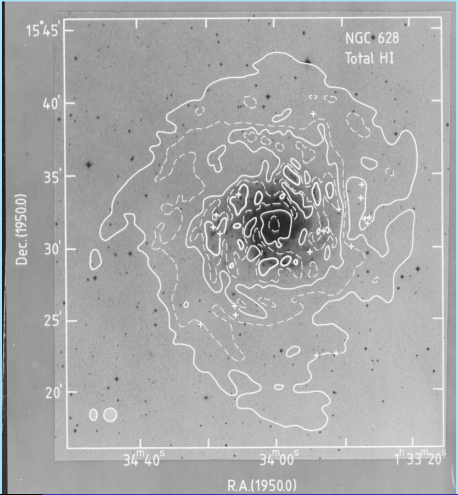

Since the disk is so close to face-on we can derive the radial distribution of the HI from simple averaging in circular annuli on the sky.

There is a feature in the profile at the edge of the stellar dsisk ($\sim$ 6 arcmin).

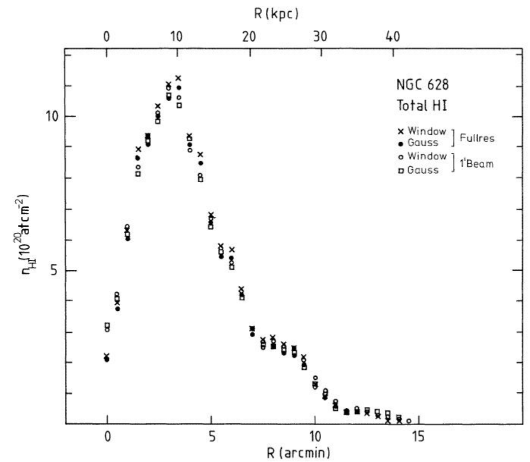

The velocity field looks regular in the central part, but has clear deviations in the outer part.

The disk is warped and the HI-plane moves actually through the plane of the sky.

At a radius of about 7 arcmin the observed velocity is about the systemic velocity.

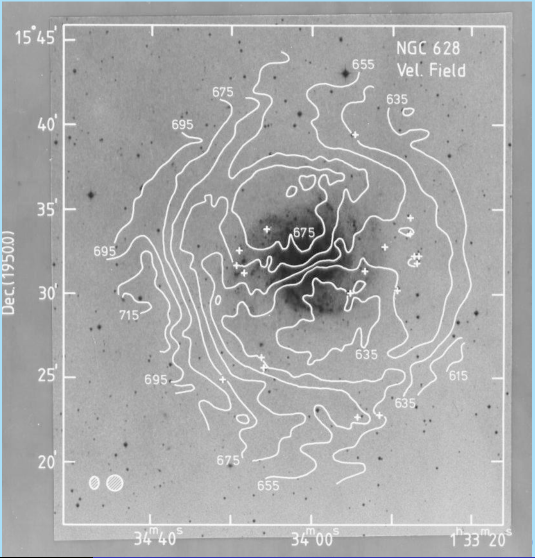

The parameters of the tilted-ring model show this also.

At about 7 arcmin the position angle moves through a large angle and the observed rotation drops to zero and then increases again.

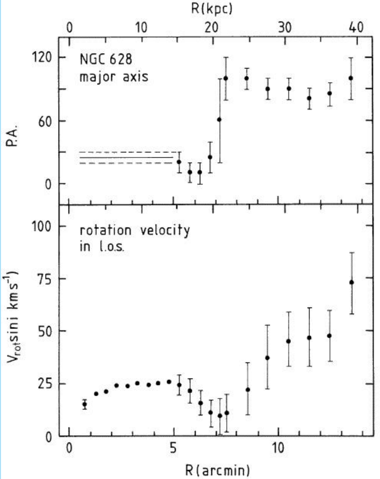

The rotation curve has an amplitude of ∼25 km/s. For a galaxy of this type and absolute magnitude (using the Tully-Fisher relation; see later) the rotation velocity should be 200 to 250 km/s.

The inclination is then only 5 to 7°.

Over the optical part we can derive the residual velocity field when that from rotation is subtracted from the observations.

This shows no systematic pattern and has an r.m.s. value of only 3.9 km/s.

Any systematic pattern of vertical motion is small (or mimic that of rotation) and the disk is therefore be extremely flat.

For comparison, in the solar neighborhood a vertical velocity of 4 km/s corresponds to an amplitude of only 45 pc.

The next thing we can do is determine the velocity dispersion of the HI.

For this we need a face-on galaxy, because the gradient of systematic motion should be small accross a beam.
Here are some individual profiles at various distances from the center.

It can be seen that Gaussians can be fit very well to these profiles.

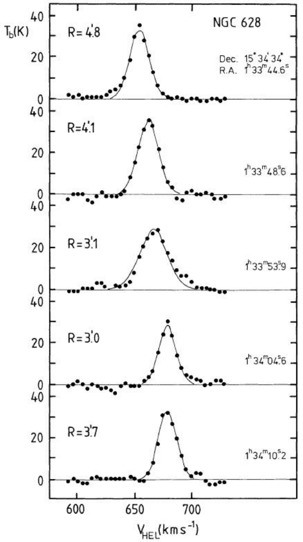

The HI velocity dispersion is between 7 and 10 km/s at all radii.

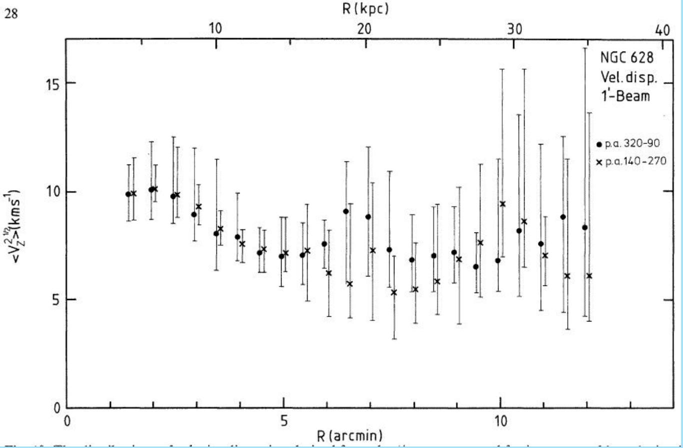

The velocity dispersion of the HI is expected to be isotropic due to cloud collisions.

This is confirmed by observations of more inclined (and large angular size) galaxies.

The value of 10 km/s corresponds roughly to a kinetic temperature of 10^4 K.

This is the temperature where cooling of the interstellar medium gets very effective due to ionisation of hydrogen.

Closer analysis shows that within the optical image the velocity dispersion is systematically higher in areas of higher surface density (the spiral arms).

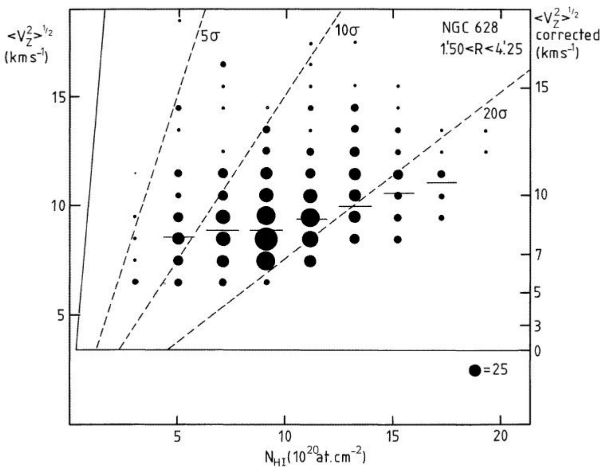

This is probably related to heating of the gas by star formation.

CO and H_2

The distribution of molecular hydrogen is often inferred from observations of CO at (sub-)millimeter wavelengths.

The assumption is that everywhere the ratio between these two molecules is the same.

This is a dubious assumption, as this ratio is very likely dependent upon metallicity and physical conditions.

Here are some observations of NGC 891[15].

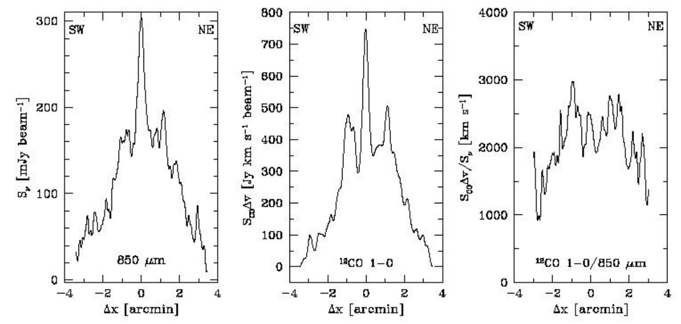

Here the near-infrared observations are also shown (these should show the distribution of the dust).

[15] F.R. Israel, P.P. van der Werf & R.J.P. Tilanus, A.&A. 334, L83 (1999)

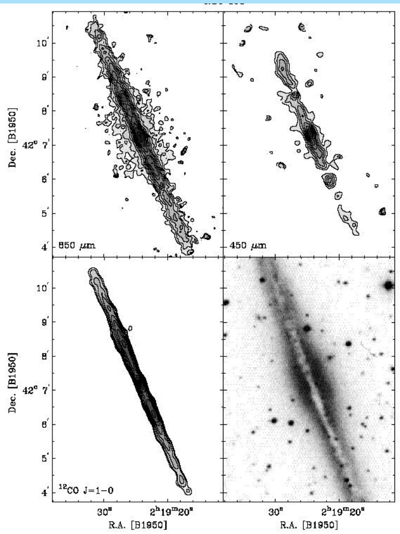
Dec. [B1950]
42° 7'
850 μm
450 μm
^{12}CO J=1−0
30s
2h19m20s
R.A. [B1950]

Only recently has it been possible to directly measure lines of H_2 with the Infrared Space Observatory (ISO)[a].

We see here observations of the S(0) (28.2 μ) (filled) and S(1) (17.0 μ) (open) lines, compared with CO-observations.

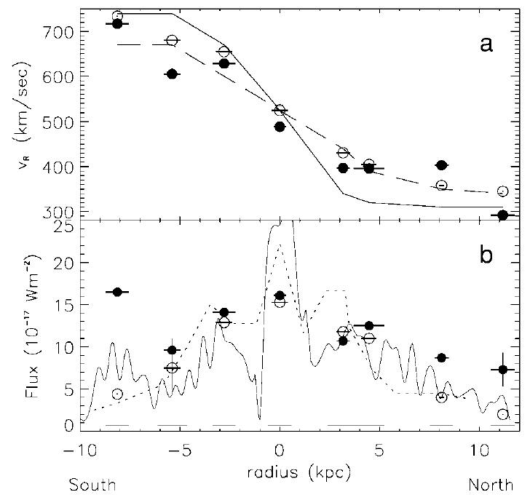

---

[a] E.A. Valentijn & P.P. van der Werf, Ap.J. 522, L29 (1999)

Stellar kinematics

To measure stellar kinematics one needs to analyse absorption line spectra.

The assumption is that the galaxy spectrum is essentially that of a late-G to early K-giant (the "template"), shifted by a radial velocity and broadened by the velocity distribution.

This is based on the fact that the integrated light from an old population is dominated by the stars in the upper part of the Giant Branch.

The fundamental equation is

$$G(\log\lambda) = \alpha\, S(\log\lambda - \delta)\, *\, B$$

$G(\log\lambda)$	=	galaxy spectrum
$S(\log\lambda)$	=	template spectrum
B	=	broadening function
δ	=	radial velocity
$\langle V^2\rangle^{1/2}$	=	velocity dispersion (the second moment of B)

Analysis is therefore exclusively based on Fourier methods[16], using:

$$\tilde{G}(k) = \gamma\, \tilde{T}(k)\cdot\tilde{B}$$

[16]Following the fundamental discussion by S.M. Simkin, A.&A. 31, 129 (1971)

Here is an example[17]

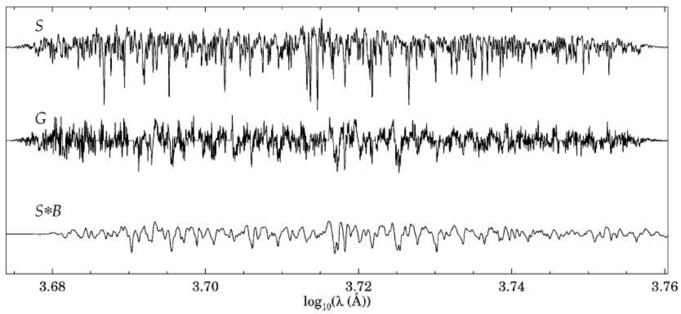

[17] From M. Kregel, P.C. van der Kruit & K.C. Freeman, Mon.Not.R.A.S. 351, 1247 (2004)

An often used part of the spectrum is around 5000Å, where one finds the Mg b triplet and many Fe I lines.

The figure below[a] shows at the top galaxy exposures and below broadened spectra of template K-giants.

[a] from van der Kruit & Freeman, Ap.J. 278, 81 (1984)

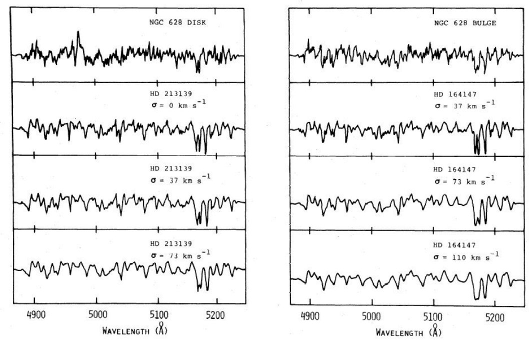

There are three general methods.

- Power spectrum method[18].
  - δ from cross-correlation peak
  - $\langle V^2 \rangle^{1/2}$ from slope of power spectrum
- Fourier quotient method[19].
  - Assume B is a Gaussian
  - Then $\tilde{B}$ is also a Gaussian (but complex)
  - Fit a Gaussian to $\tilde{G}(k)/\tilde{T}(k)$
- Cross-correlation method[20].
  - δ from cross-correlation peak
  - $\langle V^2 \rangle^{1/2}$ from width of cross-correlation peak

[18] G.D. Illingworth & K.C. Freeman, Ap. J. 188, L83 (1974)
[19] due to Paul Schechter; W.L.W. Sargent, P.L. Schechter, A. Boksenberg & K. Shortridge, Ap.J. 212, 326 (1977)
[20] J. Tonry & M. Davis, A.J. 84, 1511 (1979)